DETACHED EDDY SIMULATION OF BLADE TRAILING-EDGE CUTBACK COOLING PERFORMANCE AT VARIOUS EJECTION SLOT ANGLES

M. Effendy[1], Y.F. Yao[2*], J. Yao[3], D.R. Marchant[4]

[1] *Department of Mechanical Engineering, Universitas Muhammadiyah Surakarta, Jl. Ahmad Yani, Tromol Pos I, Pabelan, Kartasura, Surakarta 57102, Indonesia.*

[2] *Department of Engineering Design and Mathematics, University of the West of England, Coldharbour Lane, Bristol BS16 1QY, United Kingdom.*

[3] *School of Engineering, University of Lincoln, Brayford Pool, Lincoln LN6 7TS, United Kingdom.*

[4] *Faculty of Science, Engineering and Computing, Kingston University London, Penrhyn Road, Kingston upon Thames KT1 2EE, United Kingdom.*

ABSTRACT

Detached eddy simulation (DES) has been carried out to study a three-dimensional trailing-edge (TE) cutback turbine blade model with five rows of staggered circular pin-fin arrays inside the cooling passage, in order to evaluate the cooling performance in relation to coolant ejection slot angle. Simulations were performed by adopting a shear-stress transport k-ω turbulence model, and the effects of three different ejection slot angles 5°, 10° and 15° were investigated in terms of the characteristics of adiabatic film-cooling effectiveness, coefficient of discharge, and vortex shedding frequencies, respectively. The results obtained have shown that the TE cutback blade cooling with a 5° coolant ejection slot angle produced a better heat transfer coefficient than the other two ejection slot angles tested. The distributions of adiabatic film-cooling effectiveness along the cutback walls were found to be sensitive to the coolant ejection slot angle, e.g. the increase of ejection slot angle to 15^o yielded near unity of cooling effectiveness along the entire breakout walls, whereas the decrease of ejection slot angle caused a drastic decay of cooling effectiveness after the maximum effectiveness has been reached. Of the three angles studied, a TE cutback blade model with a 15° ejection slot angle produced an optimum film-cooling effectiveness. In the breakout region, vortex shedding was observed along the shear layer between the hot gas and the coolant airflow. The shedding frequencies were evaluated to be 2.93, 2.21, and 2.18 *kHz* for the ejection slot angles of 5°, 10° and 15°, respectively. The findings from this study

* Correspondence author, Yufeng.Yao@uwe.ac.uk, Tel: +44(0)1173287084

could be useful to improve existing TE cutback turbine blade design to achieve optimum film-cooling performance.

Keywords: Detached eddy simulation; Trailing-edge cutback cooling; Coolant ejection slot angle; Adiabatic film-cooling effectiveness.

Highlights

- film-cooling performance is dependent on the blowing ratio, lip-to-slot height ratio, ejection slot angle;
- film-cooling effectiveness is sensitive to the change of blowing ratio;
- vortex shedding along the breakout region is influenced by the change of blowing ratio;
- coolant ejection slot angle influences film-cooling effectiveness and discharge coefficient;
- decrease of ejection slot angle causes a drastic decay of film-cooling along the adiabatic walls.

1. Introduction

A modern gas turbine engine often operates at a higher turbine rotor inlet temperature (RIT) of up to 1,700°C. For some advanced gas turbine designs, this temperature can be further increased to a maximum value of 2000°C in an attempt to achieve the highest possible overall engine performance in terms of thermal efficiency and power output. This temperature level is obviously much higher than the melting point of the blade material, which is often below 1,000°C. Therefore, the turbine blades must be cooled both internally and externally by circulating coolant airflow from the discharged air of the compressor at around 700°C and ejecting it through pre-designed multiple arrays of cooling holes around the blade [1].

The design of an efficient cooling system for either a trailing-edge (TE) cutback or a breakout turbine blade remains a challenging problem because of its thin thickness, aerodynamic shape, the high thermal loads encountered, narrow passage geometry, combined with the need for material and structure integrity for safety and long-life operation [2]. Advanced cooling technology [3] and durable thermal barrier coatings [4][5] have played important roles for the development of

advanced gas turbines with high thermal performance. The turbine blades are usually cooled down using various internal and external cooling techniques to keep the surface temperature well below the melting point of the blade material. In fact, higher turbine inlet temperature and less effective cooling design could lead to many adverse effects such as blade deformation or partial melting, thermal stress and oxidation [6], creeping [7], corrosion [8], erosion [9], structural strength degradation, cracking [10], thermal fatigue [11][12], and buckling [13], thus increasing the risk of earlier failure of the turbine blade [14].

Commonly, a trailing-edge slot cooling is utilized as an active cooling method [15]. According to Chowdhury *et al.* [16], the performance of this kind of cooling could be evaluated based on the estimation of turbine wall temperature distribution considering a conjugate heat transfer problem that requires the simultaneous analysis of heat convection of external hot gas flow, heat conduction inside the solid blade, and heat convection of the internal cooling flow. The external convection heat transfer depends on hot gas flow along the blade, whereas the internal convection heat transfer depends on coolant flow rate and cooling passage geometry, often equipped with multiple rows of pin-fin arrays as turbulence promoters.

Internal cooling is essential to sustain the durability of components with high thermal loads such as turbine blades, where pin-fin arrays are commonly used to increase surface areas, thus providing better heat transfer performance. The pin-fin cooling, is a typical internal cooling type, usually integrated with TE ejection cooling. The co-existence of the pin-fins inside the cooling passage plays an important role in trailing-edge cooling by maintaining a high film-cooling effectiveness around the cutback or breakout blade walls [17][18] with an adiabatic wall condition.

In the past, blade trailing-edge cutback cooling models have been studied to investigate the characteristics of film-cooling along the cutback wall, which represents a key technology for improving the thermal efficiency and the power output of a gas turbine [19]. While investigating trailing-edge cutback cooling without pin-fins inside the coolant passage, Medic *et al*. [20] and Joo *et al*. [21] found that flow unsteadiness phenomenon plays an important role in turbine blade trailing-edge cutback cooling effectiveness. The streamwise vorticity in the mean flow causes the increase of heat transfer at wall surfaces. The distortion of the straight edge between the lands could significantly influence the adiabatic film-cooling effectiveness. The vortex shedding from the upper lip also has the dominant effect of flow unsteadiness, which influences the coherence of the turbulence structures and ultimately impacts on the surface heat transfer [21]. Using a similar model of TE cooling with lands, the evolutions of the turbulent flow and vortex structures with the

slot wall jets pertinent to a TE cooling of turbine blades was experimentally investigated and the results were quantified by Yang *et al*. [17][18]. The blowing ratios were found to have a significant influence on the formation of the vortex structures in the downstream region, whereas the existence of the lands contributes to the heat transfer by improving the coverage of the cooling stream over the cutback surface region. This finding was in agreement with independent research carried out by Benson *et al*. [22], who evaluated the film-cooling effectiveness due to the effect of blowing ratios and internal geometries of trailing-edge cutback. In other research, Jaswal and Ames [23] found that the effectiveness is sensitive to the change of blowing mass flow rates.

In terms of the hot gas and coolant flow mixing process behind the lip end-wall, the enhanced turbulent mixing and three-dimensional mean flow structures can further induce strong mixing and entrainment between the film-cooling slot jets and the mainstream hot gas flow [24]. Previously, Medic *et al*. [18] found that a separation bubble behind the slot lip entrains coolant flow and promotes rapid turbulent mixing at the upper edge of the coolant jet. The mean flow structures largely contribute to this rapid mixing together with a low effectiveness in fully turbulent flows [26]. Add ref [25] here] Shi *et al*. [27] noted that the variation of coolant flow can have considerable impacts on the coherent flow structures and wake behaviours. Investigation of smoothed and/or roughened cutback surfaces with various cooling models indicated that a periodically enhanced heat transfer occurs due to periodically arranged ribs and/or dimples geometry [28].

Cunha *et al*. [7][29] implemented internal pin-fin cooling geometries in a trailing-edge cutback blade that resulted in better convective thermal efficiency and heat transfer coefficient (HTC). Later, the investigation of trailing-edge cutback blades with various internal cooling features inside the cooling passage was further developed by Martini *et al*. [30] (b), who considered a layout of two rows of long ribs and pin-fins. It was found that instability of turbulent wake flow from both the lip and/or the pedestals also influences an unstable mixing process between the mainstream hot gas and the coolant airflow from the cooling passage, impacting on the film-cooling effectiveness along the cutback walls. Yuan *et al*. [31] found that the film-cooling effectiveness behind the ribs tends to be higher than other areas. An experiment using different internal structures inside a slot was also evaluated by Ling *et al*. [32]. The results showed strong horseshoe vortices formed around the blockages of the slots, which resulted in non-uniform coolant flow on the breakout surface and in the near wake region.

The design of internal cooling obstacles with a circular and/or an elliptic pin-fin geometry feature has been experimentally evaluated by Horbach *et al*. [33]. From this evaluation it was found that the internal blockage of the cooling passage causes a strong decrease in both the discharge coefficient and the film-cooling effectiveness, while the heat transfer coefficient increases significantly along the cutback walls. In particular, an elliptical fin-pin geometry will have a strong effect on the discharge behaviour as well as the effectiveness of the film-cooling and heat transfer. Previously, Choi *et al*. [34] found that the design of the internal geometry of a trailing-edge and the flow Reynolds number can influence the heat transfer in an internal passage model with a perforated blockage insertion. Both long pedestals and ribs in a TE blade cooling system were also evaluated by Beniaiche *et al*. [35]. A comprehensive numerical study was performed by Gao *et al*. [36], who focused on unsteady flow characteristics and the film-cooling effectiveness in a blade trailing-edge cutback region, referring to those configurations investigated previously by Martini *et al*. [37][30].

In addition, an extra coolant airflow from an internal cavity was ejected through the cooling holes in the vicinity of the cutback slots in order to fulfil the required cooling effectiveness in the downstream region of a TE cutback blade [38][39]. Furthermore, other research has been undertaken to evaluate the dynamics of coherent structures on the blade pressure side (PS) film-cooling due to the existence of cooling holes and a cutback slot. The flow behind the lip end-walls tends to be dominated by the counter clockwise vortex of the cooling flow side [40]. This vortex grows around the holes and further develops into a periodic pattern up to the cutback lip [41].

The need for careful design of the coolant ejection of the blade trailing-edge cutback cooling has been recognised by the industry, but somehow the understanding of the physical flow and precise quantification of cooling performance have not yet been achieved. To the authors' knowledge, there are few publications in the public domain that deal with the effect of ejection slot angle on a TE cutback blade cooling, as most researchers merely evaluated the performance of blade TE cooling at a fixed ejection slot angle. For example, Yuan *et al*. [31] investigated experimentally the film-cooling of a trailing-edge within a fixed coolant ejection slot angle of 0°, while both Martini *et al.* [30][37][42] and Horbach *et al*. [33] considered an ejection slot angle of 10° in their experiments. Schneider *et al*. [43][44] also used the 10° ejection slot angle in their numerical studies. Furthermore, each researcher utilized different models and geometries in their studies, so there is a lack of uniformity for objective fair comparisons and assessments.

One experimental study has been evaluated the film-cooling effectiveness downstream of trailing edge slots. The study considered the effects of density ratio, slot width and lip thickness, including the impact of ejection slot angle change between 0 and 15° [45]. Despite the fact that other conditions were not in the typical operating range of a modern turbine blade, the results revealed that a trailing-edge breakout cooling with an 8.5° ejection slot angle was an optimum angle for producing the best film-cooling effectiveness. Inspired by this work, the present study considers realistic gas turbine operating conditions to evaluate the effect of ejection slot angle on the blade TE cooling performance.

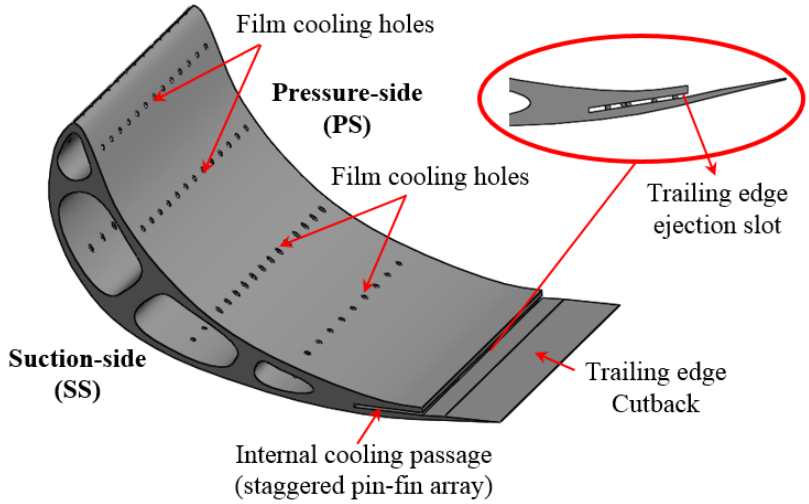

Figure 1: Sketch of a blade TE cutback cooling.

In order to further advance the TE cutback cooling studies discussed above, three different ejection slot angles (5°, 10° and 15°) are proposed in the simulation. The study is a continuation of research that has been successfully accomplished and published [46], with the design impact of lip thickness (t). Figure 1~~Figure 1~~ illustrates a sketch of a TE cutback turbine blade cooling with five rows of staggered circular pin-fin arrays used in the present study. By keeping the same ratio of lip thickness-to-slot (t/H) at 1, a computational domain of TE cutback cooling with three coolant ejection slot angles (α) was carefully designed by rotating the coolant slot of the L_1 region and the cutback/breakout wall of the L_3 region with regard to the reference axis of z = 0, whilst the slot-height (H) is kept constant at 4.8 mm (see Figure 2~~Figure 2~~(a)). The length of the slot-exit in the vertical direction (H_{se}) is slightly increased by approximately 2.7% when changing the ejection slot angle from 5° to 15°. This means the cross-section area of the slot-exit is slightly widened due to the increase of ejection slot angle. The slot-exit area reduces to 1.15% if the ejection slot angle decreases from 10° to 5°, whilst it increases 1.54% if the ejection slot angle increases from 10° to

15°, as summarised in Table 1. Therefore, the coolant airflow may vary by a few percent when ejecting coolant air through the slot-exit for the design with a higher ejection slot angle. This variation is small therefore its impact on results is considered to be negligible.

Table 1: The key dimensions of the slot-exit area.

α (degree)	t/H	t (mm)	H (mm)	H_{se} at the slot-exit	Area (mm^2) at the slot-exit
5	1.0	4.8	4.8	4.818	57.816
10	1.0	4.8	4.8	4.874	58.488
15	1.0	4.8	4.8	4.949	59.388

2. Numerical Treatment

Detached eddy simulation (DES) is a hybrid method of combining Reynolds-averaged Navier Stokes (RANS) and large-eddy simulation (LES), which offers an efficient and effective approach for predicting three-dimensional unsteady turbulent flow and heat transfer phenomena, particularly for separated flows. The governing equations of contemporary DES are based on an SST k-ω turbulence model as described by Effendy *et al*. [46].

2.1 Computational domain and boundary conditions

Figure 2~~Figure 2~~ shows a computational domain of a trailing-edge cutback turbine blade model with five rows of staggered circular pin-fin arrays. The arrays are fitted in various wedge-shaped ducts from 5 to 15 degrees as described in Table 1, replicating the typical trailing edge shape of a gas turbine blade. The cutback region along L_3 ($0 < x/H < 12$) as an investigated challenging area is in parallel to the slope of the coolant ejection slot angle (α) formed by a wedge-shaped duct at the L_1 region. In the coolant duct, spanwise pitch (S/D) and streamwise pitch (S_x/D) are kept the same ratio as the experiment. The ratio of lip thickness to coolant passage height (t/H) was 1. The coolant ejection area that known as the slot-exit (A_{slot}) is located under the lip position.

In order to reduce computational cost, the domain in this simulation considered a distance of two pitchwise ($2S$) in the spanwise z-direction, and only half a corresponding wind tunnel height (i.e. H_{hg} = 52.5 mm) in the vertical y-direction, corresponding to the parameters used in the previous computational studies (see, e.g. [46]). This computational domain was chosen after some precursor

validation exercises between results from one pitch wise (S) and two pitch wise ($2S$) in terms of discharge coefficient and adiabatic film-cooling effectiveness. The physical property change along the upper surface was also checked during the validation stage.

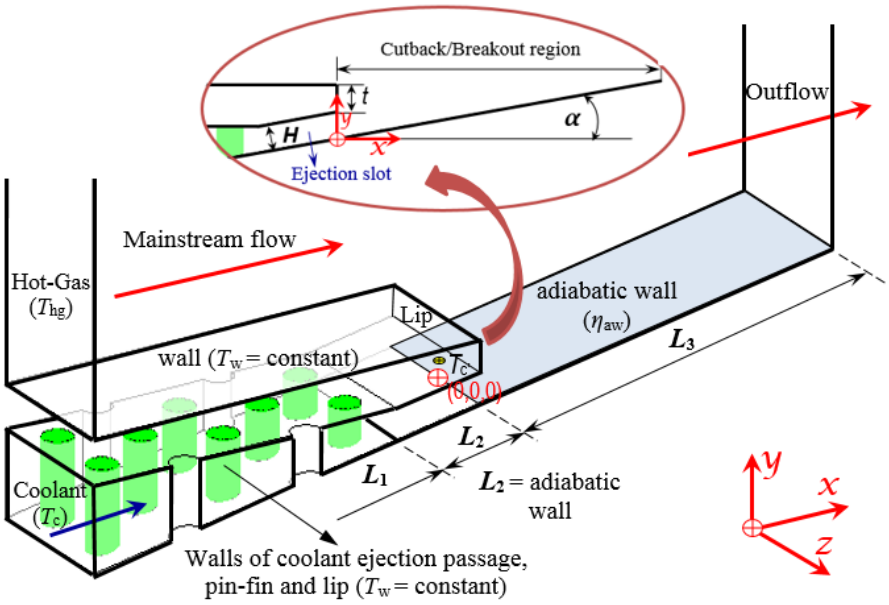

(a). 3D view of computational domain with boundary condition

Dimensions	L_1	L_2	L_3	S	S_x	t	H	D	α
mm	52	14.4	60	12	10.4	4.8	4.8	4.8	5-15°

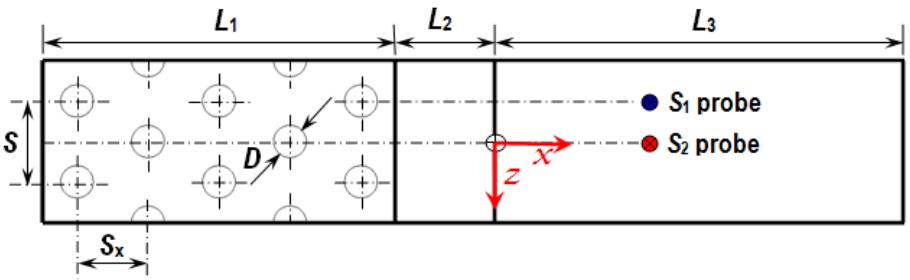

(b). Top view of computational domain with geometry

Figure 2: Computational configurations. (a) side-view; (b) 3D-view.

The inflow and boundary conditions are the same as those used in previous experimental studies suggested by Martini *et al*. [30] to evaluate the heat transfer coefficient on the pin-fin wall surfaces inside the cooling passage, the discharge coefficient across the cooling passage, the blade TE film-cooling effectiveness at the cutback wall surfaces, the vortex shedding frequency and dynamic mixing between the mainstream hot gas and the coolant airflow, respectively. The mainstream flow conditions were set at a fixed velocity (u_{hg}) of 56 m/s and temperature (T_{hg}) of 500 K. The

coolant inflow condition was set at a temperature (T_c) of 293 K, while the coolant velocity (u_c) was varied from 4 to 15 *m/s*, corresponding to a blowing ratio (M) from 0.5 to 1.1. Table ~~Table~~ 2 provides a summary of the numerical test conditions used in the study.

Table 2: The numerical test conditions.

	Mainstream flow (hot gas)	Coolant flow
Velocity [*m/s*]	u_{hg} = 56	u_c = 4 - 15
Temperature [*K*]	T_{hg} = 500	T_c = 293
Turbulence Intensity [*%*]	Tu_{hg} = 7	Tu_c = 5
Length Scale [*mm*]	10	1.5

2.2 Mesh generation

Figure 3~~Figure 3~~ illustrates the 3D multi-block structured meshes of the computational domain and the front views of the structured meshes around the lip region for three different ejection slot angles. The local mesh generation at the lip and ejection slot area in the *x-y* plane can be seen from Figure 3~~Figure 3~~(b) - Figure 3~~Figure 3~~(d). The difference of ejection slot angle is evident by the slope change of the lower wall. The lip and slot-height ratio (t/H) is designed to maintain the same value to facilitate objective comparisons. The detailed 3D view of the meshes can be seen in [46]. The multi-block structured grids were created using the Gambit meshing tool, with finer meshes clustered around the wall surfaces and mesh sizes growing away from the wall with the growth of mesh spacing away from the walls in all three directions, as suggested by Joo *et al*. [21]. The boundary layer meshes were applied to all wall surfaces to ensure sufficient spatial resolution of $\Delta y^+ < 1$ was achieved. In order to guarantee the quality of meshes, all models were constructed by keeping the same topology and the block number as the baseline model with an ejection slot angle of 10^o. The consistency of local grid spacing in the 3D domain was refined in all three *x*, *y* and *z* directions in order to have a sufficiently fine spatial resolution to capture unsteady flow phenomenon in the mixing region. **Error! Reference source not found.**~~Table~~ 3 gives a comparison of mesh statistics for the three cases studied.

Table 3: Mesh statistics.

Ejection slot angles (α)	5°	10° (baseline)	15°
Inside the cooling passage region			
pin-fin wall [a] Δy_1^+	0.784	0.907	1.010
end-wall Δy_1^+	0.555	0.749	0.984
Mainstream region			

pressure side wall Δy_1^+	0.488	0.482	0.477
lip wall Δy_1^+	0.539	0.607	0.724
TE cutback/breakout region			
Number of elements, $n_x \times n_y \times n_z$	124×48×48	124×48×48	124×48×48
cutback wall Δy_1^+	0.183	0.257	0.320
average			
Δy_1^+	0.613	0.740	0.876

[a] an average of Δy_1^+ in the radial direction of pin-fins, [b] elements at the block of breakout-slot region

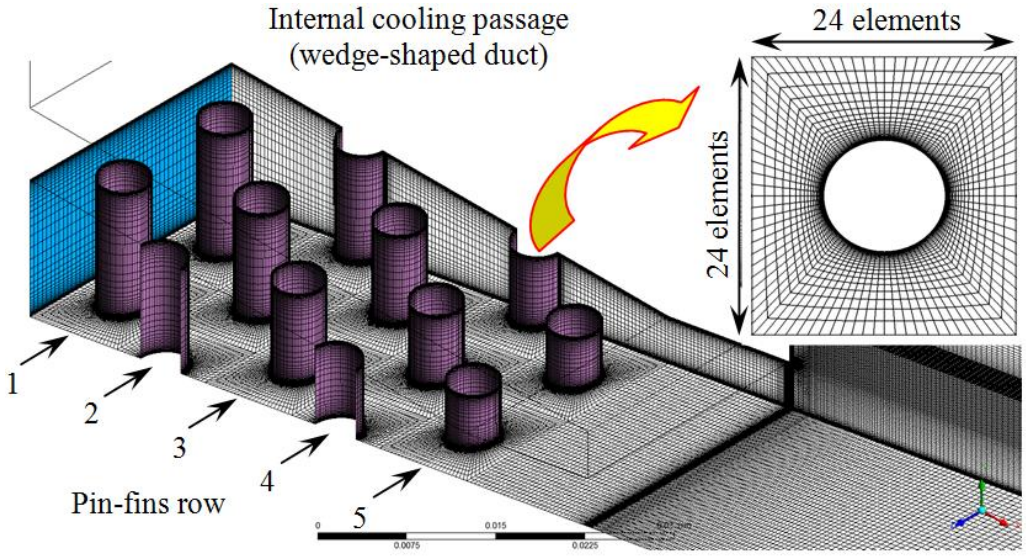

(a) The 3D structured meshes, inserted by the local 2D structured meshes around the pin-fin

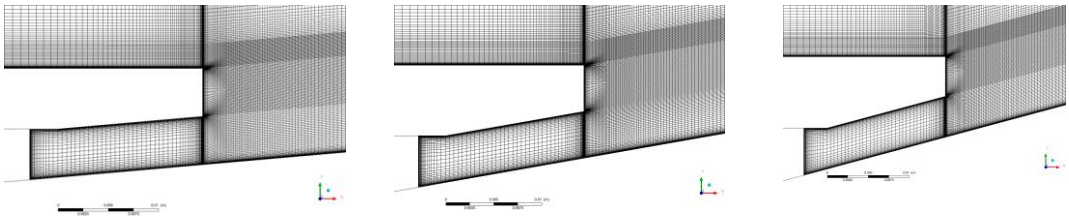

(b) α = 5° (c) α = 10° (d) α = 15°

Figure 3: The 3D multi-block structured meshes of computational domain and 2D meshes snapshots at three different ejection slot angles.

2.3 Solution algorithm and time-step for transient flow

A finite-volume method was utilised to solve the governing equations of low-speed incompressible flows. The Semi-Implicit Method for Pressure-Linked Equations Consistent (SIMPLEC) algorithm was chosen by applying a second-order numerical scheme for all flow equations (i.e. pressure, momentum, and energy). Furthermore, for DES calculations, not only the grid size, but also the time-step must be small enough to satisfy the stability criteria and to ensure a sufficiently fine temporal resolution in an attempt to account for the unsteady flow effects. Considering all

these requirements, a small time-step of 1.25 × 10^{-5} seconds, as used in previous studies, was adopted to realise unsteady vortex shedding phenomena for frequency analysis [46].

Figure 4~~Figure 4~~ provides the iteration history of the simulations for the three different case studies. The collected data is based upon the centre point (Tc'_2) temperature at the slot-exit under the lip, where the same temperature will be used to calculate the adiabatic film-cooling effectiveness. It can be seen that all three cases have been simulated for sufficiently long enough to reach a statistically converged status in order to gain time averaged results. After that, the computations were continued for a further 2000 time steps to collect statistics.

For the case with a 10° ejection slot angle, after approximately 11,000 iterations the simulation exhibited some oscillations; whereas, after approximately 8,000 iterations the other two simulations tended to be a near constant 'flat' level. The observed oscillation could be partly attributed to the growth of turbulence levels when ejecting coolant airflow from the slot exit. This iteration history also shows that the level of temperature for the ejection slot angle of 5° is lower than that of the other two cases.

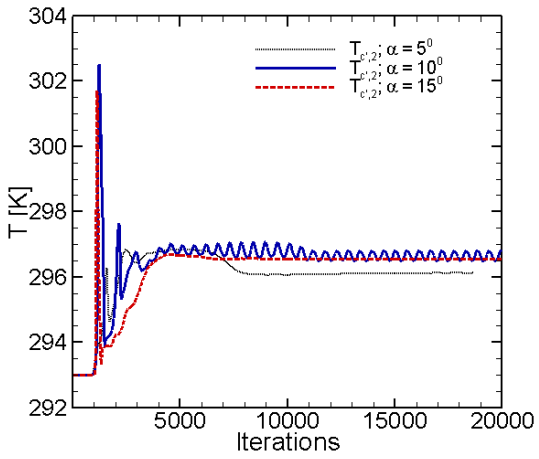

Figure 4: Simulation History.

2.4 Validation

Figure 5~~Figure 5~~ shows the DES predicted discharge coefficient (C_D) and the adiabatic film-cooling effectiveness ($\overline{\eta}_{aw}$) along the TE cutback wall surfaces, respectively, in comparison with the experimental data for various blowing ratios (M). The validation data was obtained by using the block-structured finer meshes as shown in Figure 3~~Figure 3~~. More details about the grid refinement studies can be found in reference [46].

Blowing ratio. The non-dimensional blowing ratio (M) is defined as a factor of slot-averaged mean density and velocity product over the density and velocity product at the main hot gas inlet plane. The equation can be further transformed using the mass flow rate at the slot exit, which is equal to that of the cooling inlet (i.e. mass conservation).

$$M = \frac{\overline{(\rho_c u_c)}_{slot}}{\rho_{hg} u_{hg}} = \frac{\dot{m}_c}{A_{slot} \rho_{hg} u_{hg}}, \tag{1}$$

Discharge Coefficients. The discharge coefficient, C_D, is a representation of the global pressure losses inside the cooling passage, which is defined by the measured coolant mass flow over the ideal mass flow as formulated below

$$C_D = \frac{\dot{m}_{c,real}}{\dot{m}_{c,ideal}}, \tag{2}$$

$$C_D = \frac{\dot{m}_{c,real}}{p_{1,t} \cdot \left(\frac{p_2}{p_{1,t}}\right)^{\frac{\kappa+1}{2\kappa}} \cdot A_{slot} \cdot \sqrt{\frac{2\kappa}{(\kappa-1) \cdot R \cdot T_{1,t}} \left[\left(\frac{p_{1,t}}{p_2}\right)^{\frac{\kappa-1}{\kappa}} - 1\right]}} \tag{3}$$

where $p_{1,t}$ and $T_{1,t}$ are the total pressure and temperature at the coolant inlet, respectively, p_2 is the static pressure at the slot exit, A_{slot} is the area of the slot exit, κ is the specific heat capacity and R is the gas constant.

From Figure 5~~Figure 5~~(a), it can be seen that the predicted discharge coefficients for blowing ratios (M) of 0.5, 0.8 and 1.1 are in good agreement with the available measurement data. The change of blowing ratio is proportional to the change of the coolant mass flow rate. The discharge coefficient is found to increase slightly by increasing the blowing ratio. This finding is in agreement with the works of Martini *et al.* [30][37] and Horbach *et al.* [33], who confirmed that the coefficient of discharge is increased by raising the Reynolds number of the coolant flow.

Film-cooling effectiveness. The performance of trailing-edge cutback cooling is commonly expressed by film-cooling effectiveness along the breakout wall from the slot-exit and downstream region. If the surface of TE cutback is with the adiabatic wall condition, the film-cooling effectiveness can be derived from the ratio of temperature difference between the hot gas and the wall surface to the temperature difference between the hot gas and the coolant gas as given in equation (4);

$$\eta_{aw} = \frac{T_{hg} - T_{aw}}{T_{hg} - T_{c'}}, \quad (4)$$

where T_{aw} is the temperature at the adiabatic wall surfaces, T_{hg} is the hot gas temperature at the mainstream flow at the inflow region and $T_{c'}$ is the coolant gas temperature measured at the centre of the slot-exit between two neighbouring pin-fins

Figure 5~~Figures 5~~(b)-5(d) clearly demonstrate that the present DES modelling is capable of predicting this key performance parameter, with the noticeable and important cooling effectiveness decay phenomena around *x/H* = 3 being captured accurately. The adiabatic film-cooling effectiveness data along the breakout/cutback walls (L_3) are presented, in comparison with both previous experimental measurements for the baseline model with a fixed *t/H* ratio of 1.0. Similarly, simulations using the baseline specimen are in good agreement for all three various blowing ratios, compared to both the experimental data obtained by previous researchers [30][33]. From Figure 5~~Figure 5~~(c), a slight increase of film-cooling effectiveness is clearly seen in the downstream region of *x/H* > 3 for the experiment data at *M = 0.95*. It is likely that this is due to an anomalous phenomenon at a blowing ratio of 0.95, as noted in a previous experiment by Horbach *et al*. [33]. The adiabatic film-cooling effectiveness tends to grow up to a higher level, compared to the case of a higher blowing ratio of 1.1. The adiabatic film-cooling effectiveness tends to drop by increasing the blowing ratio from *M* = 0.8 to 1.25. In the meantime, the decrease of CFD predicted film-cooling effectiveness is likely caused by intensified vortex shedding from the ejection lip. This occurs within a certain operating range with the slot ejection, leading to an intensified mixing process between the coolant flow and mainstream hot gas. Comparing the validation data of the film-cooling effectiveness from Figure 5~~Figure 5~~(b) – Figure 5~~Figure 5~~(d), the vortex flow structure at a higher blowing ratio seems to have more effect on the mixing process than counter-rotating vortex pairs found predominantly at a lower blowing ratio, as addressed in [44].

Based on the validation of both key performance parameters as illustrated in Figure 5~~Figure 5~~, it could be concluded that they are acceptable for further detailed investigations by focusing on three different ejection slot angles (5°, 10° and 15°) of TE cutback blade cooling configurations.

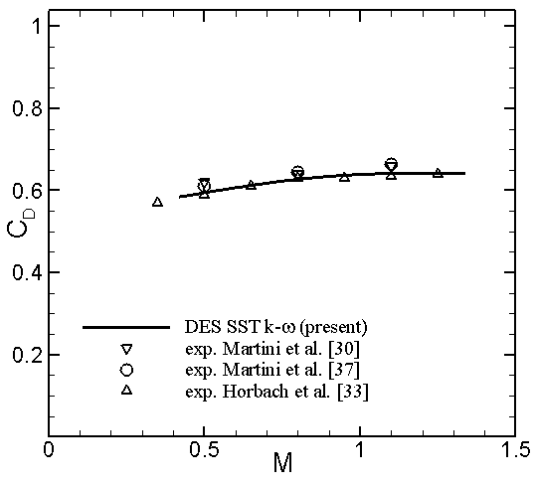

(a) Discharge coefficient

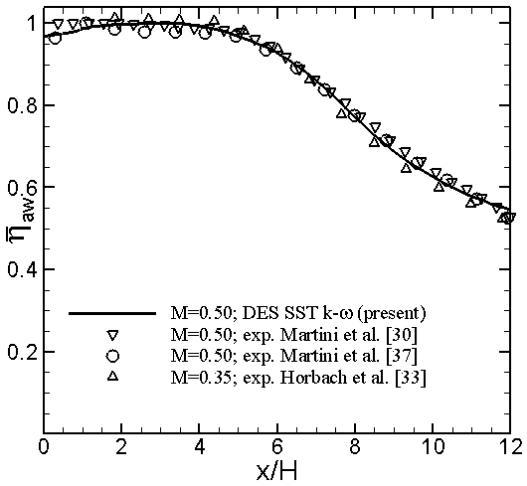

(b) Adiabatic film-cooling effectiveness at $M = 0.5$

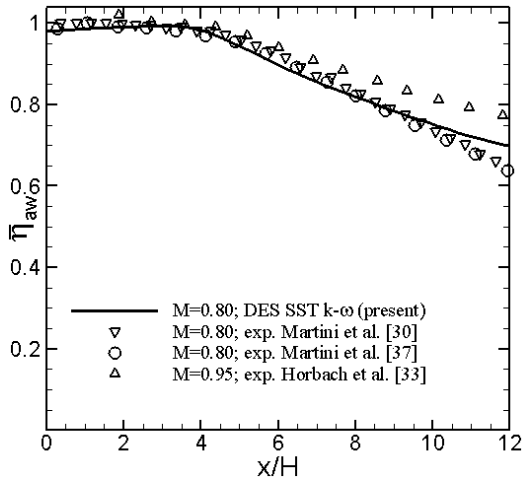

(c) Adiabatic film-cooling effectiveness at $M = 0.8$

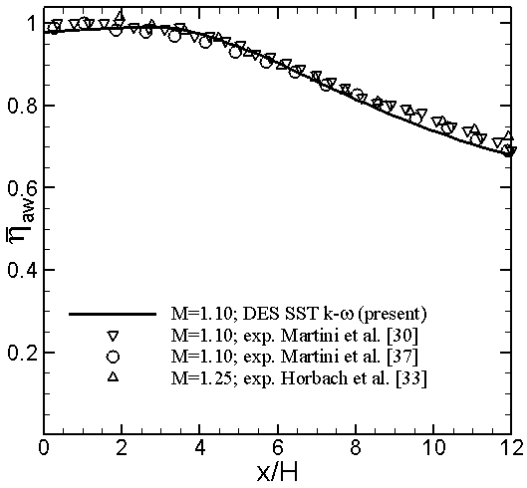

(d) Adiabatic film-cooling effectiveness at $M = 1.1$

Figure 5: Validation studies.

3. Results and Discussion

The computations of blade TE cutback cooling were performed for three different coolant ejection slot angles. The results and discussion are presented below by starting with the coolant flow behaviour inside the cooling passage, and then followed by the performance of the blade TE cutback cooling. The dynamic interactions between the mainstream hot gas and the coolant flow, including the frequency spectrum, will be discussed thereafter.

3.1 Discharge coefficient

Figure 6~~Figure 6~~ shows the predicted data of discharge coefficient (C_D) from three different ejection slot angles, compared to the experimental measurements by Martini *et al*. [30] and

Horbach *et al*. [33], respectively. The CFD predicted data are plotted against the blowing ratio. The results show that the increase of ejection slot angle (α) from 5° to 15° causes the increase of discharge coefficient at a given blowing ratio. The deviation is more pronounced between the two ejection slot angles of 5° and 10°, compared to those of 10° and 15°. The discharge coefficient can be reduced by up to 21.31% when the coolant ejection slot angle is changed from 10° to 5°, whereas it can be increased by about 9.63% when the angle is changed from 10° to 15°.

The lowest discharge coefficient is found for a configuration with 5° coolant ejection slot angle which is most likely caused by a larger pressure drop inside the cooling passage. As the pin-fin height reduces with the decrease of the coolant ejection slot angle, this implies the reduction of the pin-fins surface area and the cross section area inside the cooling passage close to the inflow region. Moreover, both the inlet and the slot exit sections have almost the same section area when a blade trailing-edge cutback is designed with a coolant ejection slot angle of 0°. As previously mentioned, the rise of coolant ejection slot angle will cause a slight increase in the slot-exit area (see Table 1). This illustrates that the change of coolant ejection slot angle influences geometry changes for the inlet region in terms of, the pin-fin height, the slot-exit height, and the inclination of the cutback wall surfaces. The change of these geometries will collectively influence the overall pressure loss inside the cooling passage and therefore impact on the discharge coefficient.

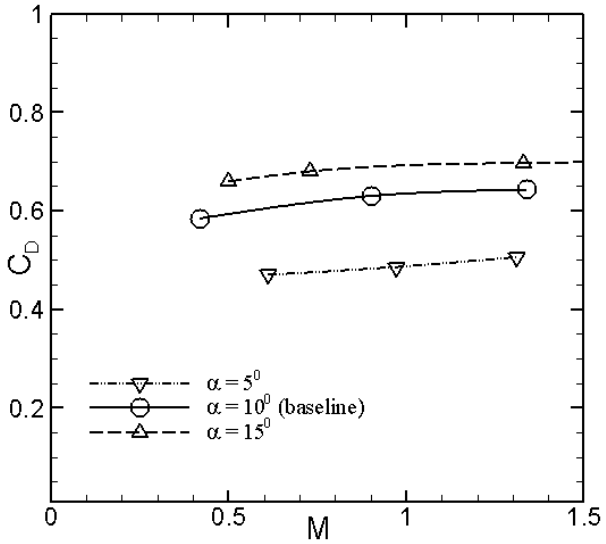

Figure 6: Discharge coefficient.

As previously stated, the CFD data for the baseline model agrees well with the available experimental data for the same design with a coolant ejection slot angle of 10°. This means both CFD and experimental methods yield the same trend data at three different blowing ratios. Based on this coefficient, it can be concluded that the increase of ejection slot angle causes the increase

of discharge coefficient, thus the power need of a coolant flow could be less due to the reduction of the pressure loss in the cooling passage.

3.2 Coolant properties inside the cooling passage

Figure 7~~Figure 7~~(a) shows the quantitative coolant properties at the surface of the pin-fin arrays for the three cases studied. This is the averaged data at the pin-fin surfaces of each row of arrays. The row position of the pin-fin arrays from P_1 to P_5 refers to the inserted picture in Figure 7~~Figure 7~~(a). It is found that the HTC at the pin-fin surfaces inside the internal cooling passage has moderate increments row-by-row. The peak HTC occurs in the fifth row, then it tends to further decrease (for an ejection slot angle of 5°) or increase (for ejection slot angles of 10° and 15°). Hwang *et al*. [47] have found a similar trend in their study using a trapezoidal-duct, where the highest HTC occurs at the third pin-fin row, then reduces afterwards. In addition, the increase of HTC is likely caused by an acceleration effect due to the wedge-shaped duct of the cooling passage [48]. A stronger flow interaction in both streamwise and spanwise directions also contributes to the HTC change. The intensity of turbulent wake shedding illustrates a good correlation of the heat transfer coefficient in the wakes of the pin-fins.

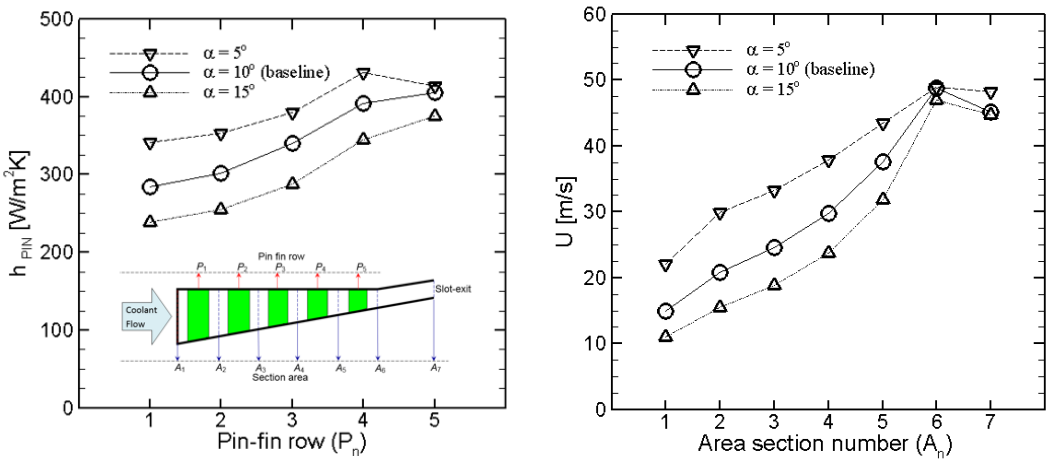

(a) Heat transfer coefficient (b) Velocity

Figure 7: Coolant properties inside the cooling passage.

An experimental study by Tarchi *et al*. [49] found that the pin-fin HTC in a wedge-shaped duct tends to reduce after the fourth row of the pin-fin arrays. Using a parallel duct, Goldstein and Chen [50] recognised that the pin-fin HTC increases from the first row to the second row and then remains near constant after the third row. The results from the present numerical study are in agreement qualitatively with those investigations. A study by Metzger *et al*. [51] of the heat

transfer coefficient through ten rows of staggered arrays within a parallel duct has found that the HTC discrepancy can be up to 12% between the highest and the lowest values.

As listed in Table 4, the HTC on the pin-fin surface (h_{PIN}) is always greater than on the end-walls (h_{EW}), with a discrepancy about 53 – 58%. This finding is consistent with the work of Tarchi *et al.* [49]. Both h_{PIN} and h_{EW} values increase up to 12.7% when the ejection slot angle is decreased to 5°, and after that the ratio of h_{PIN}/h_{EW} remains in a range between 1.53 and 1.58. By contrast, HTC drops by about 13.36% when the ejection slot angle is increased from 10° to 15°. According to Liao *et al*. [52], the junctions of the pin–fins and the end-walls cause complicated vortex structures which consequently influence the end-wall heat transfer rates. This means that the change of ejection slot angle influences the flow characteristics at its junction, which is correlated to vortex structures formed around the pin-fins. Further detail about vortex structures around the pin-fin in a rectangular cooling channel was discussed by Moon and Kim [53].

The increase of HTC is likely caused by the combined effect of flow acceleration and intensifying flow interactions along the wedged-duct passage. The turbulence flow intensity becomes stronger due to the existence of pin-fin arrays, which influence the heat transfer process. The wake flow shedding downstream of the stagnation point causes the increase of heat transfer near the trailing-edge of the pin-fin as addressed by Ames *et al*. [54]. A gradual increase in heat transfer is obvious for the second row, while a sharp increase is more pronounced between the second and the fourth rows. This trend of development is similar to that observed by Ames *et al*. [55] who used eight rows of staggered arrays in their studies.

Table 4: The comparison of predicted HTC.

Ejection slot angle (α)	$h_{PIN}\,(W/m^2K)$	$h_{EW}\,(W/m^2K)$	h_{PIN}/h_{EW}
5°	369.0322	240.1240	1.5368
10°	331.2857	209.2242	1.5834
15°	283.5324	184.7391	1.5348

Figure 7~~Figure 7~~(b) illustrates some discrepancies of the coolant flow velocity before approaching the ejecting slot as indicated at the cross-section area number A_6. The discrepancy is likely due to the geometry change of a wedge-shaped duct at the L_1 region at different ejection slot angles. This change to the geometry causes different turbulence levels which will influence the characteristics of the coolant flow velocity along the wedge-shaped duct. The decrease of ejection slot angle causes the reduction of a wedge-shaped duct, mainly at the inlet region. This affects the

construction of the fitted pin-fin arrays and coolant flow velocity, which then increases the turbulence level as seen in Figure 8. In addition, a staggered array of pin-fins can influence the interactions between the horseshoe vortices and wake flows in such a complex three-dimensional flow problem [50].

3.4 Turbulence characteristics

Figure 8~~Figure 8~~ gives the characteristics of turbulence levels (T_u = u'/U_∞) inside the cooling passage and along the blade TE cutback cooling for three coolant ejection slot angles. The u' velocity is based on a root-mean-square (RMS) streamwise flow fluctuation velocity. It was found that for all three cases the T_u gradually increased inside the cooling passage of a wedge-shaped duct. Both the averaged-turbulence levels at the cross-section areas (A_n) and at the pin-fin surfaces (P_n) recognise its increase ('n' is the number of row or cross-section). The increase becomes more obvious in the fluid region, as the T_u at the cross-section areas is greater than at the pin-fin surfaces. It is also more profound near the slot exit (A_7), particularly for the design with a 5° ejection slot angle.

This development of turbulence levels is similar to the trend observed by Ames *et al.* [55] who studied the eight row staggered arrays of pin-fins in a flat duct with various inlet flow rates. They reported finding the T_u value to be in a range of 0.014 – 0.203 for *Re = 3,000* flow. The present research has also found that the T_u value is less than 0.2 along the wedge-shaped duct. The change of ejection slot angle from 15° to 5° would decrease the overall $T_{u.}$ values inside the coolant passage.

Further observations for three different data positions at the z/H = 0, 0.625 and 1.25 have shown that the T_u fluctuates inside the cooling passage, due to the effect of the pin-fin arrays. It becomes more noticeable at the stagnation point and in the wake of the pin-fins. The construction of the pin-fins promotes the vortex formations and reverse flow phenomenon which causes the turbulence intensity behind the pin-fins to be greater than in the front of the pin-fins. The horseshoe vortices and wakes interact with each other, producing a complex three-dimensional flow problem. This higher turbulence intensity level is also related to the vortex recirculation (i.e. lateral vortex) behind the pin-fin arrays. These wakes causes the cooling fluids to become 'trapped' inside each pin–fin backflow region and thus forms lower heat transfer regions there. In addition, the wake flow shedding influences the heat transfer process in the pin-fin arrays.

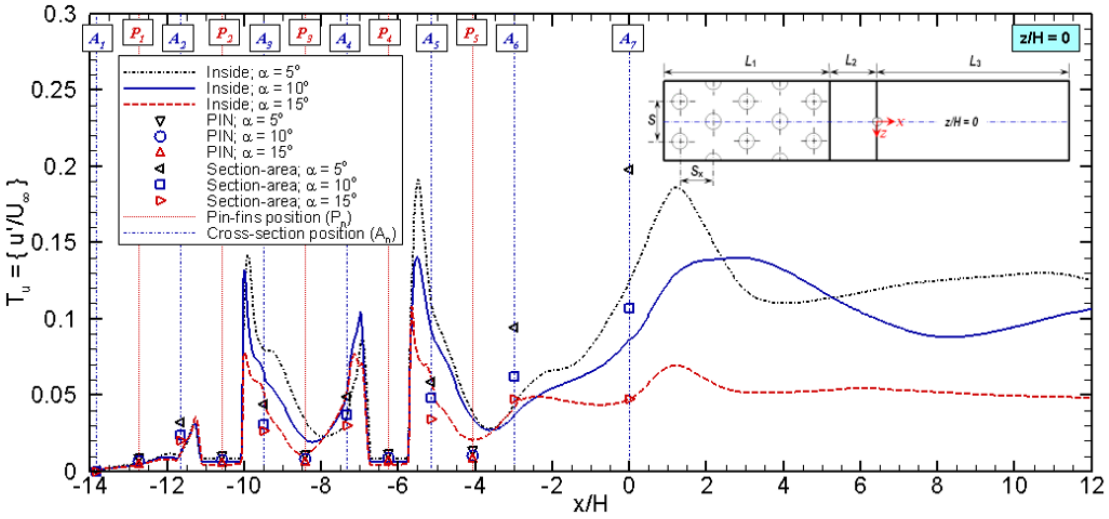

(a) $z/H = 0$

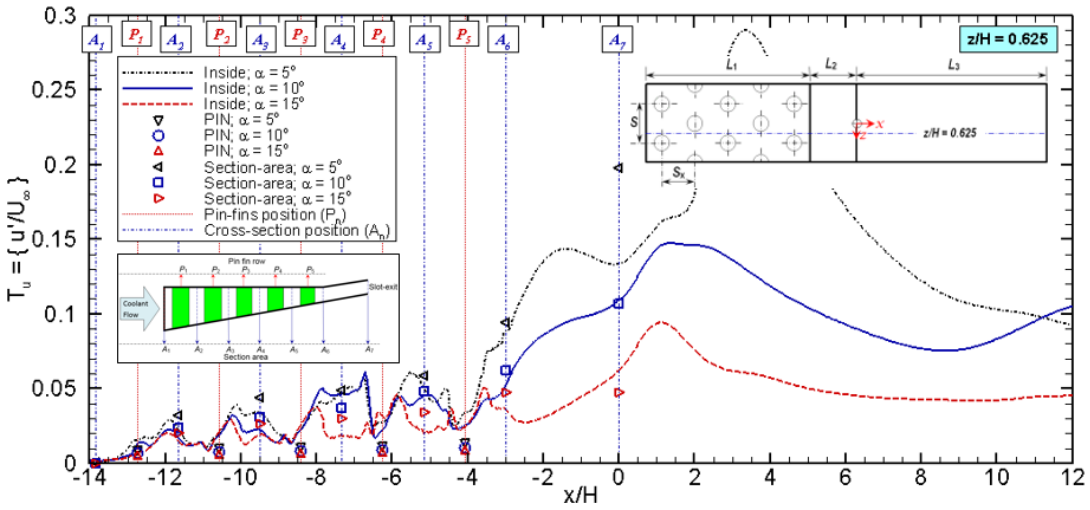

(b) $z/H = 0.625$

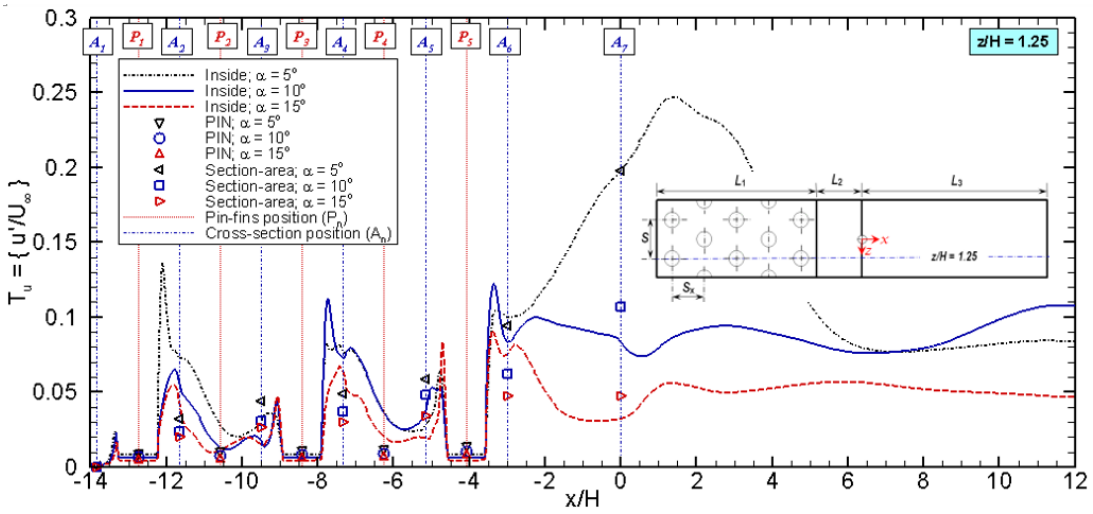

(c) $z/H = 1.25$

Figure 8: Turbulence levels.

According to Axtmann *et al*. [56], flow across the internal cooling passage can be characterized by pin-fin wake and horseshoe vortices. Additionally, the typical topology of flow around the pin-fins array could be corner vortex, the secondary vortex, tertiary vortex and von Karman Vortex Street. All types of vortex will contribute towards a complexity of flow around the pin-fins which influences flow unsteadiness along the coolant passage ($-14 < x/H < 0$). The fluctuation of the T_u indicates an accumulation of vortices being formed which implicate the existence of flow unsteadiness up to the downstream region.

As seen in Figure 8~~Figure 8~~, the turbulence level increases rapidly with the increase of an ejecting coolant at the slot exit (A_7), and then decreases after approaching the peak value behind the lip region. It is more obvious for the design with a 5° ejection slot angle. In addition, the turbulence level grows bigger along the mixing region where a dynamic interaction between the mainstream hot gas and the coolant air flow ejection occurs. This may be attributed to the turbulent flow structures along the mixing region ($0 < x/H < 12$), and finally influences the adiabatic film-cooling effectiveness on the TE cutback cooling blade.

3.5 Laterally averaged film cooling effectiveness

Figure 9~~Figure 9~~(a) shows a quantitative comparison of the adiabatic film-cooling effectiveness at three ejection slot angles, in comparison with two previous experiments by Martini *et al*. [30] and Horbach *et al*. [33], respectively. The CFD predicted data of the baseline model at a blowing ratio of 1.1 agrees well with both experiments, while the design with a 15° ejection slot angle yields the highest performance as indicated by the adiabatic film-cooling effectiveness reaching near unity along the cutback wall surfaces ($0 < x/H < 12$). A slight decay is observed after approaching a peak level at $x/H = 8$.

Conversely, the design with 5° ejection slot angle generates a fast decay of the adiabatic film-cooling effectiveness after attaining a position of $x/H > 3$. The deviation is clearly seen near the slot-exit region of $0 < x/H < 4$, with a discrepancy up to 2.12% compared to the other two angles. This decay is likely to be caused by a rapid increase of temperature at the cutback wall surfaces, which will have a direct influence on the calculation of the adiabatic film-cooling effectiveness. This implies that the effectiveness follows the temperature change at the cutback wall surfaces.

Figure 9~~Figure 9~~(a) shows that the increase of ejection slot angle improves the performance of TE cutback cooling as indicated by the highest level of effectiveness up to the downstream region.

This confirms that the coolant ejection slot angle is one of the key parameters in determining the quality of the cooling film at the cutback wall in the TE cutback cooling design.

Figure 9~~Figure 9~~(b) presents temperature at the cutback wall surface which has a direct link with the adiabatic film-cooling effectiveness shown in Figure 9~~Figure 9~~(a). Both figures display opposite trends and this temperature discrepancy is likely influenced by the different mixing process between the mainstream hot gas and coolant airflow, which seems to affect the 'penetration' of the mainstream hot gas into the near wall region of the cutback TE blade. It also relates to the turbulence flow structures at the breakout region due to the effect of the diverse generation of unsteady vortex shedding behind the blunt lip, as previously addressed by Schneider *et al*. [44]. The unsteadiness of flow mixing has also been discussed in the previous section by illustrating the intensity of turbulence level (see, e.g. Figure 8~~Figure 8~~). It is clearly seen that the turbulence level for the design with a 15° ejection slot angle remains 'steady' at the lowest level, compared to the other two angles, which tend to fluctuate more along the mixing region ($0 < x/H < 12$). This causes the adiabatic film-cooling effectiveness at the cutback wall to reach near unity.

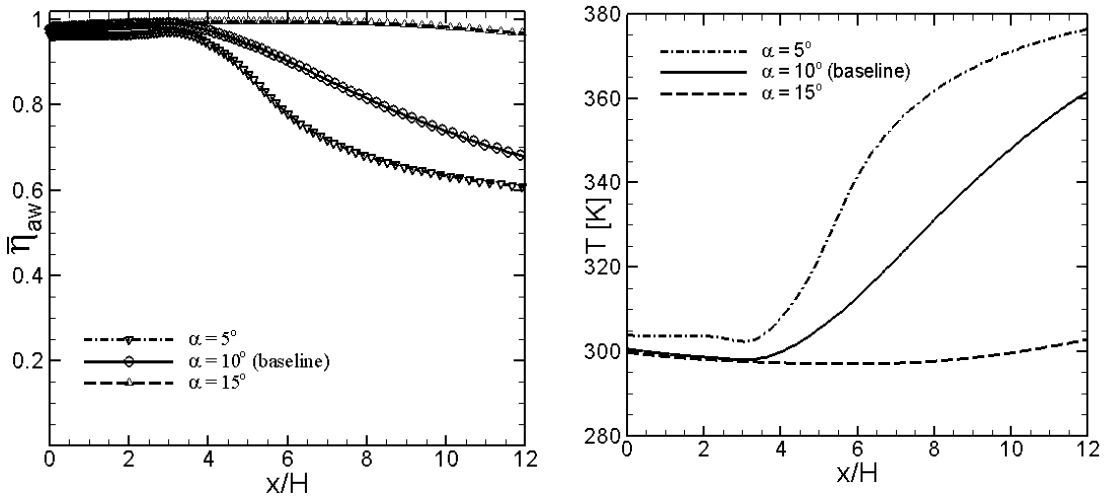

(a) Adiabatic film-cooling effectiveness (b) End-wall temperature

Figure 9: Laterally averaged data at the cutback wall at a selected blowing ratio of 1.1.

3.6 Turbulent flow structures and normalized time-averaged velocity

As discussed above, the cooling performance of a trailing-edge cutback blade is likely related to the coherent structures in the mixing region. Figure 10~~Figure 10~~ (the left-hand-side) shows the side view of the turbulent flow structures in the mixing region for three ejection slot angles, superimposed by contours of the adiabatic film-cooling effectiveness at the cutback walls (η) and (the right-hand-side) the streamline of normalized flow velocity (U/U_{hg}) from the mainstream and

the coolant flows in the *x-y* plane for a fixed position of z/H = -1.25. The turbulent flow structures are presented by iso-surfaces of the vortex identification criterion $Q = 0.5(\Omega^2 - S^2)$ as used by Terzi *et al*. [57] and Schneider *et al.* [17] [43], respectively. The iso-surfaces are coloured by the average temperature of thermal mixing, from a low value of 293 *K* (in blue colour) to a high value of 500 *K* (in red colour), whereas the flow velocity is scaled from a low value of 0 (in blue colour) to a high value of 1 (in red colour).

Figure 10~~Figure 10~~ (the left-hand-side) shows that the change of the coolant ejection slot angle has a significant impact on the formation of turbulent flow structures in the mixing region. The TE cutback cooling design with a 15° ejection slot angle significantly affects the film-cooling at the cutback wall surface, as seen in a region $0 < x/H < 12$. The shielded film-cooling almost dominates the whole cutback surfaces, as indicated by blue colour in Figure 10~~Figure 10~~(c) (the left-hand-side figure).

The domination is diminished by reducing the ejection slot angle from 15° to 10°. By comparing Figure 10~~Figure 10~~(b) and Figure 10~~Figure 10~~(c), it can be see that the blue colour narrows moderately for the design with a 10° ejection slot angle. This is due to the wakes formed at this angle being larger than the design with the 15° ejection slot angle, which enhances the penetration of mainstream hot gas flow into the cutback wall, mainly near the downstream region (see region $6 < x/H < 12$). Therefore, a decay of the adiabatic film-cooling effectiveness is noticeable as shown in Figure 9~~Figure 9~~.

Figure 10~~Figure 10~~ (the right-hand-side figures) gives the normalized time-averaged velocity (U/U_{hg}) in the mixing region at the *x-y* plane for a fixed position z/H = 0. This is presented by the shade of colour applicable to the velocity vector, from a low value of 0 (in blue colour) to a high value of 1 (in red colour). It is found that the generation of unsteady vortex-shedding is most likely influenced by the periodic wake flow from the coolant slot, which depends on the coolant ejection slot angle. It seems to become more 'flat' in the downstream region for the design with a higher ejection slot angle. In contrast, the velocity fluctuation is more obvious for the design with the lower ejection slot angle.

As previously discussed (see Figure 9~~Figure 9~~), the computation for the design with a 15° ejection slot angle yields the adiabatic film-cooling effectiveness of near unity along the cutback wall surface. The increase of ejection slot angle is seen to disrupt the penetration of the mainstream hot gas into the cutback wall surface due to flow interactions between the mainstream hot gas and

coolant airflow occurring at a point closer to the lip. An interaction between both flows near the lip could cause an inclined flow concentration, where the hot gas flow over the lip wall forms a vortex behind the lip and the hot gas flow away from the lip tends to keep the coolant thin-layer film near the cutback wall in the downstream region. Continuous cooling supply from the exit slot forms a thin-layer of film-cooling that can be maintained near the end-wall surfaces.

Ω^2 - S^2 at the mixing region

U/U_{hg} at the x-y plane of z/H = 0

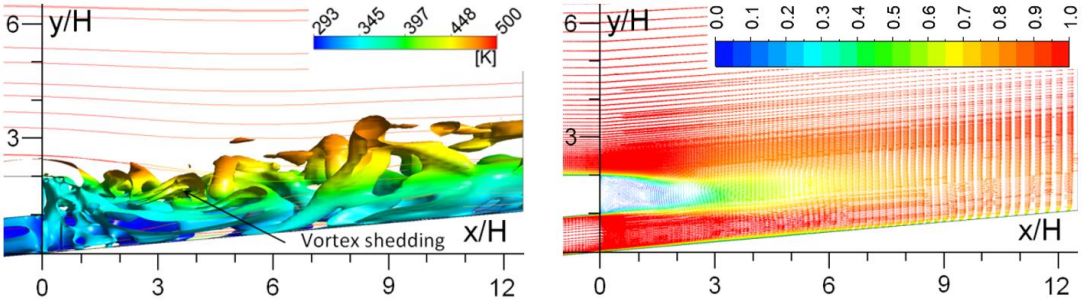

(a) α = 5°

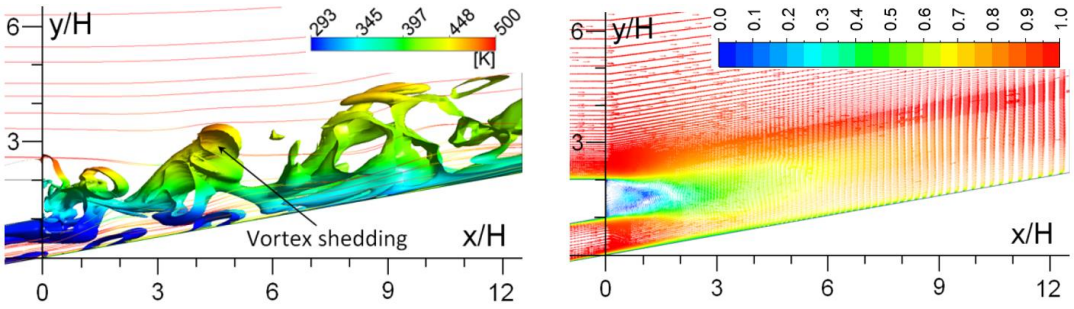

(b) α = 10°

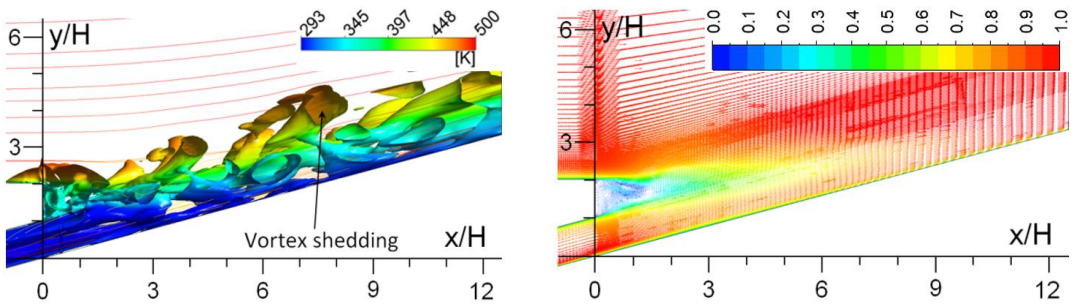

(c) α = 15°

Figure 10: Turbulent flow structures ($\Omega^2 - S^2$) and normalized time-averaged velocity (U/U_{hg}).

It is noted that there is difference from the design with a 5° ejection slot angle which allows an interaction of the mainstream hot gas and the coolant airflow to occur at a range further downstream from the lip. Certainly, the difference in the mixing process causes the different growth of vortex shedding along the mixing region. Finally, it causes a strong penetration of the mainstream hot gas to influence the heat transfer process in the downstream region. The shielded film cooling at the cutback surface appears to be shorter than for the other two ejection slot angles, due to a stronger influence of the mainstream hot gas flow.

According to Schneider *et al*. [19], a distinct large coherent structure promotes the generation of strong turbulent heat flux, which causes a significant enhancement of the thermal mixing process in the near-wall region that is concomitant with the excessive decay of the film cooling effectiveness. Similarly, Effendy *et al.* [46] also found the growth of vortices with longer wave lengths induces a strong mixing between the mainstream hot gas and the coolant airflow, which degrades the cooling film effectiveness.

3.7 Shedding frequency

Figure 11~~Figure 11~~ shows the shedding frequencies of a mixing flow over the TE cutback cooling which illustrates the dynamic characteristics of the mixing between mainstream hot gas and coolant airflow for three ejection slot angles. These frequencies were analysed by fast Fourier transformation (FFT) based on a sampled dataset of mixing flow velocities at two different monitoring points, as defined in Figure 2~~Figure 2~~(b) at S_1 location (x/H = 4, y/H = 1.5, z/H = 1.25) and S_2 location (x/H = 4, y/H = 1.5, z/H = 0), respectively The resultant velocities were recorded from each case of simulation after a statistically converged status, in a selected time range of 0.019 - 0.025 *s*.

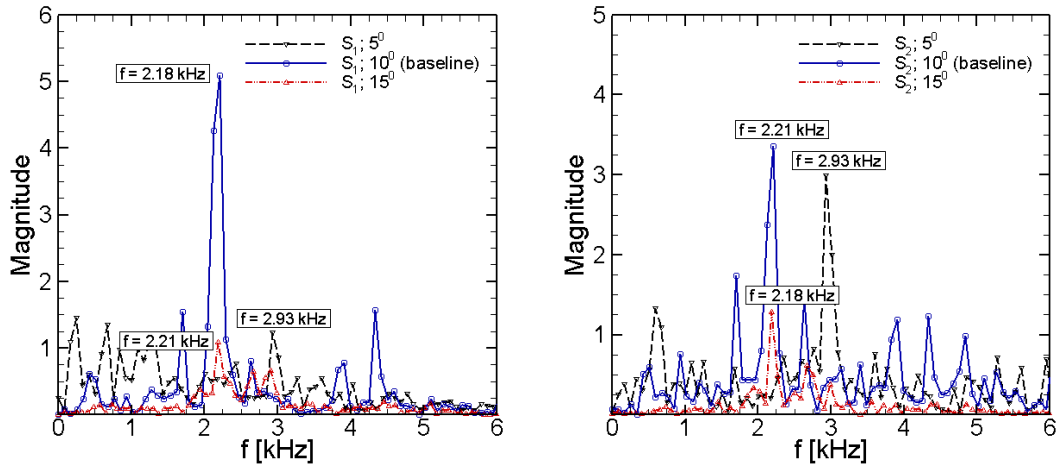

(a) S_1 monitoring point (b) S_2 monitoring point

Figure 11: Shedding frequencies.

It was found that the dominant spectrum frequencies are f_s = 2.93, 2.21, and 2.18 *kHz* for the TE cutback cooling at the ejection slot angles α = 5°, 10° and 15°, respectively. There is no major discrepancy of dominant frequency at both monitoring points. However, each point has a slight difference in terms of the magnitude. The magnitude of the dominant frequency resulting from the design with a 15° ejection slot angle is lower than that for the other two angles. The magnitude of monitoring points S_1 is overall less than at S_2. (see Figure 2~~Figure 2~~) This discrepancy is most likely due to the effect of the pin-fin arrays inside the cooling passage which influence the growth of vortex shedding along the cutback region. The TE cutback cooling with an ejection slot angle of 10° is found to be in good agreement with the available data obtained by Martini *et al*. [30], who reported dominant frequencies at 2.36 *kHz* and 2.4 *kHz* with a computational approach and an analytical calculation, respectively.

From Figure 11, it can be seen that the beating phenomenon occurs with harmonic and sub-harmonic waves being formed in normal patterns. It has the appearance of harmonic motion inside an envelope within a certain period. The forcing frequency of both turbulent flow motion from the mainstream hot gas and the coolant airflow may have a natural frequency close to the unsteady mixing flow along the cutback region. As found by Medic *et al*. [20], sub-harmonic response appears in all cases they have studied. In the present study, the sub-harmonics are found to be very pronounced for the design with the coolant ejection slot angle of 10°.

4. Conclusion

The blade TE cutback cooling at three coolant ejection slot angles has been investigated numerically by DES with SST *k-ω* models. Turbulent flow structures have been captured together

with vortex shedding that provides underlying evidence regarding the cooling performance. The findings can be summarized as follows:

- The increase of coolant ejection slot angle causes the increase of discharge coefficients, indicating decreased pressure loss along the cooling passage;
- The blade TE cutback cooling with a small coolant ejection slot angle of 5° generates a higher level of the heat transfer coefficient for the pin-fin cooling. In contrast, the decay of the adiabatic film-cooling effectiveness is more pronounced due to the effect of the intensified mixing process between the mainstream hot gas and the coolant airflow.
- The distribution of the adiabatic film-cooling effectiveness at the cutback wall is found to be sensitive to the coolant ejection slot angle. The increase of ejection slot angle yields the cooling effectiveness near to unity almost along the breakout wall, whereas the decrease of ejection slot angle causes a drastic decay of cooling effectiveness after approaching the peak level.
- The shedding frequencies are predicted as 2.93, 2.21, and 2.18 *kHz* for the blade TE cutback cooling at three ejection slot angles of 5°, 10° and 15°, respectively, which is in good agreement with published work.

5. Acknowledgments

The first author would like to acknowledge the financial assistance provided by the Indonesian Government to support the research through Universitas Muhammadiyah Surakarta.

6. Nomenclature

A_{slot} = Area at slot exit [m^2]

A_n = Position of cross-section areas

C_D = Discharge coefficient ($C_D = \frac{\dot{m}_{c,real}}{\dot{m}_{c,ideal}}$)

D = Pin-fin diameter [mm]

f_s = Shedding frequency [kHz]

H = Slot-height [mm]

H_{se} = Slot-height at the slot-exit [mm]

h = Heat transfer coefficient [W/m^2K]

$L_{1,2.3,4}$ = Streamwise lengths of the domain [*mm*]

M = Blowing ratio ($M = \frac{\overline{(\rho_c u_c)}_{slot}}{\rho_{hg} u_{hg}} = \frac{\dot{m}_c}{A_{slot} \rho_{hg} u_{hg}}$)

$\dot{m}_c$ = Mass flow rate of coolant air [*kg/s*]

n_x; $n_{y;}$ n_z = Element number in the *x*, *y*, and *z* directions, respectively

P_{hg} = Pressure of hot gas [*kPa*]

P_n = Position of pin-fins row

$P_{1,t}$ = Total pressure at the coolant inlet [*kPa*]

P_2 = Static pressure at the slot-exit [*kPa*]

Q = Vortex identification criterion

R = Ideal gas constant (R = 287.22 *J/kg.K* for air)

S = Pitch-wise distance of the ribs array [*mm*]

S_x = Streamwise distance of the ribs array [*mm*]

S_1 = First monitoring point location

S_2 = Second monitoring point location

T_{aw} = Temperature at the adiabatic wall surfaces [*K*]

T_c = Coolant air temperature [*K*]

$T_{c'}$ = Coolant air temperature measured at the centre of the slot-exit [*K*]

T_{hg} = Hot gas temperature [*K*]

T_u = Turbulence level

T_w = Isothermal wall temperature [*K*]

$T_{1,t}$ = Total temperature at the coolant inlet [*K*]

t = Lip thickness of blade trailing-edge cutback [*mm*]

u = Velocity [*m/s*]

u’ = A root-mean-square streamwise fluctuation flow velocity [*m/s*]

U_∞ = Mainstream hot gas velocity [*m/s*]

u_c = Coolant air velocity [*m/s*]

u_{hg} = Hot gas velocity [*m/s*]

x, y, z = Cartesian coordinates

Greek Symbols

α = Inclined angle of suction-side [degree] or an ejection slot angle [°]

ρ = Density of airflow [kg/m^3]

κ = Specific heat capacity

ρ_c = Coolant air density [kg/m^3]

ρ_{hg} = Hot gas density [kg/m^3]

η_{aw} = Adiabatic film cooling effectiveness ($\eta_{aw} = \frac{T_{hg} - T_{aw}}{T_{hg} - T_{c'}}$)

$\overline{\eta}_{aw}$ = Averaged adiabatic film cooling effectiveness

Subscripts

aw = Adiabatic wall

cg = Coolant gas (air)

c’ = Coolant gas (air) at the slot exit

hg = Hot gas

n = Number

s = Shedding-vortex

se = Slot-exit

Abbreviations

DES = Detached eddy simulation

EW = End-wall

FFT = Fast Fourier transformation

HTC = Heat transfer coefficient

LES = Large-eddy simulation

PIN = Pin-fins

PS = Pressure-side

RANS = Reynolds-averaged Navier-Stokes

RIT = Rotor inlet temperature

RMS = root-mean-square

SS = Suction-side

SST = Shear-Stress Transport

TE = Trailing-edge

7. References

[1] J.-C. Han, “Fundamental Gas Turbine Heat Transfer,” *Therm. Sci. Eng. Appl.*, vol. 5, no. 2,

p. 21007, 2013.

[2] A. Murata, K. Yano, M. Hanai, H. Saito, and K. Iwamoto, “Arrangement Effects of Inclined Teardrop-shaped Dimples on Film Cooling Performance of Dimpled Cutback Surface at Airfoil Trailing–edge,” *J. Heat Mass Transf.*, vol. 107, pp. 761–770, 2017.

[3] J.-C. Han, “Advanced Cooling in Gas Turbines 2016 Max Jakob Memorial Award Paper,” *J. Heat Transfer*, vol. 140, no. 11, p. 113001, 2018.

[4] A. B. Moskalenko and A. I. Kozhevnikov, “Estimation of Gas Turbine Blades Cooling Efficiency,” *Procedia Eng.*, vol. 150, pp. 61–67, 2016.

[5] M. S. Sahith, G. Giridhara, and R. S. Kumar, “Development and Analysis of Thermal Barrier Coatings on Gas Turbine Blades - A Review,” *Mater. Today Proc.*, vol. 5, no. 1, pp. 2746–2751, 2018.

[6] R. Becchi, B. Facchini, A. Picchi, L. Tarchi, D. Coutandin, and S. Zecchi, “Film Cooling Adiabatic Effectiveness Measurements of Pressure Side Trailing–edge Cooling Configurations,” *J. Propuls. Power Res.*, vol. 4, no. 4, pp. 190–201, 2015.

[7] F. J. Cunha and M. K. Chyu, “Trailing-Edge Cooling for Gas Turbines,” *J. Propuls. Power*, vol. 22, no. 2, pp. 286–300, 2006.

[8] N. Eliaz, G. Shemesh, and R. M. Latanision, “Hot Corrosion in Gas Turbine Components,” *Eng. Fail. Anal.*, vol. 9, no. 1, pp. 31–43, 2002.

[9] Y. Q. Xiao, L. Yang, Y. C. Zhou, Y. G. Wei, and N. G. Wang, “Dominant Parameters Affecting the Reliability of TBCs on a Gas Turbine Blade during Erosion by a Particle-laden Hot Gas Stream,” *Wear*, vol. 390–391, pp. 166–175, 2017.

[10] Y. S. Choi and K. H. Lee, “Investigation of Blade Failure in a Gas Turbine,” *Mech. Sci. Technol.*, vol. 24, no. 10, pp. 1969–1974, 2010.

[11] M. Beghini, L. Bertini, C. Santus, B.D. Monelli, E. Scrinzi, N. Pieroni, and I. Giovannetti, “High Temperature Fatigue Testing of Gas Turbine Blades,” *Procedia Struct. Integr.*, vol. 7, pp. 206–213, 2017.

[12] W. Maktouf and K. Saï, “An Investigation of Premature Fatigue Failures of Gas Turbine Blade,” *Eng. Fail. Anal.*, vol. 47, pp. 89–101, 2015.

[13] A. L. Brundage and M. W. Plesniak, “Experimental Investigation of Airfoil Trailing–edge Heat Transfer and Aerodynamic Losses,” *Exp. Therm. Fluid Sci.*, vol. 31, pp. 249–260, 2007.

[14] T. J. Carter, “Common Failures in Gas Turbine Blades,” *Eng. Fail. Anal.*, vol. 12, pp. 237–247, 2005.

[15] J. Ling, C. J. Elkins, and J. K. Eaton, “Optimal Turbulent Schmidt Number for RANS Modeling of Trailing Edge Slot Film Cooling,” *Eng. Gas Turbines Power*, vol. 137, pp. 1–8, 2018.

[16] N. H. K. Chowdhury, H. Zirakzadeh, and J. Han, “A Predictive Model for Preliminary Gas Turbine Blade Cooling Analysis,” *J. Turbomach.*, vol. 139, pp. 1–12, 2018.

[17] Z. Yang and H. Hu, “Study of Trailing-Edge Cooling Using Pressure Sensitive Paint Technique,” *J. Propuls. Power*, vol. 27, no. 3, pp. 700–709, 2011.

[18] Z. Yang and H. Hu, “An Experimental Investigation on the Trailing–edge Cooling of Turbine Blades,” *J. Propuls. Power*, vol. 1, no. 1, pp. 36–47, 2012.

[19] H. Schneider, D. Von Terzi, and H. Bauer, “Turbulent Heat Transfer and Large Coherent Structures in Trailing-edge Cutback Film Cooling,” *Flow Turbul. Combust.*, vol. 88, pp. 101–120, 2012.

[20] G. Medic and P. Durbin, “Unsteady Effects on Trailing–edge Cooling,” *J. Heat Transfer*, vol. 127, no. 4, p. 388, 2005.

[21] J. Joo and P. Durbin, “Simulation of Turbine Blade Trailing–edge Cooling,” *Fluids Eng.*, vol. 131, no. 2, p. 21102, 2009.

[22] M. J. Benson, C. J. Elkins, S. D. Yapa, J. B. Ling, and J. K. Eaton, “Effects of Varying Reynolds Number, Blowing Ratio, and Internal Geometry on Trailing Edge Cutback Film Cooling,” *Exp. Fluids*, vol. 52, no. 6, pp. 1415–1430, 2012.

[23] I. Jaswal and F. E. Ames, “Letterbox Trailing–edge Heat Transfer : Effects of Blowing Rate, Reynolds Number, and External Turbulence on Heat Transfer and Film Cooling Effectiveness,” *J. Turbomach.*, vol. 132, pp. 1–10, 2018.

[24] Y. Chen, C. G. Matalanis, and J. K. Eaton, “High Resolution PIV Measurements around a Model Turbine Blade Trailing–edge Film-cooling Breakout,” *Exp. Fluids*, vol. 44, no. 2, pp. 199–209, 2008.

[25] M. J. Benson, C. J. Elkins, and J. K. Eaton, “Measurements of 3D Velocity and Scalar Field for a Film-cooled Airfoil Trailing Edge,” *Exp. Fluids*, vol. 51, no. 2, pp. 443–455, 2011.

[26] M. Benson, S. D. Yapa, C. Elkins, and J. K. Eaton, “Experimental-Based Redesigns for Trailing–Edge Film Cooling of Gas Turbine Blades,” *J. Turbomach.*, vol. 135, no. 4, p. 41018, 2013.

[27] L. L. Shi, S. C. Yao, and R. Dai, “Coherent Structures in the Wake behind a Trailing–edge Cutback,” *Exp. Therm. Fluid Sci.*, vol. 94, pp. 329–344, 2018.

[28] A. Murata, S. Nishida, H. Saito, K. Iwamoto, Y. Okita, and C. Nakamata, “Effects of Surface Geometry on Film Cooling Performance at Airfoil Trailing–edge,” *J. Turbomach.*, vol. 134, pp. 1–8, 2013.

[29] F. J. Cunha, M. T. Dahmer, and M. K. Chyu, “Analysis of Airfoil Trailing Edge Heat Transfer and Its Significance in Thermal-Mechanical Design and Durability,” *J. Turbomach.*, vol. 128, pp. 700–748, 2006.

[30] P. Martini, A. Schulz, H.-J. Bauer, and C. F. Whitney, “Detached Eddy Simulation of Film Cooling Performance on the Trailing–edge Cutback of Gas,” *J. Turbomach.*, vol. 128, pp. 292–299, 2006.

[31] Y. Hepeng, Z. Huiren, and K. Manzhao, “Effects of Blowing Ratio Measured by Liquid Crystal on Heat Transfer Characteristics of Trailing–edge Cutback,” *Chinese J. Aeronaut.*, vol. 21, no. 6, pp. 488–495, 2008.

[32] J. Ling, M. J. Benson, C. J. Elkins, and J. K. Eaton, “Three-Dimensional Velocity and Scalar Field Measurements of an Airfoil Trailing–edge With Slot Film Cooling : The Effect of an Internal Structure in the Slot,” *J. Turbomach.*, vol. 135, pp. 1–8, 2013.

[33] T. Horbach, A. Schulz, and H. Bauer, “Trailing–edge Film Cooling of Gas Turbine Airfoils — External Cooling Performance of Various Internal Pin Fin Configurations,” *J. Turbomach.*, vol. 133, pp. 1–9, 2011.

[34] J. Choi, S. Mhetras, J.-C. Han, S. C. Lau, and R. Rudolph, “Film Cooling and Heat Transfer on Two Cutback Trailing–edge Models With Internal Perforated Blockages,” *J. Heat Transfer*, vol. 130, no. 1, p. 12201, 2008.

[35] A. Beniaiche, C. Carcasci, M. Pievaroli, and A. Ghenaiet, “Nusselt Correlations in a Trailing–edge Cooling System with Long Pedestals and Ribs,” *Energy Procedia*, vol. 45, pp. 1067–1076, 2014.

[36] Y. Gao, X. Yan, J. Li, and K. He, “Investigations into Film Cooling and Unsteady Flow Characteristics in a Blade Trailing–edge Cutback Region,” *J. Mech. Sci. Technol.*, vol. 32, no. 10, pp. 5015–5029, 2018.

[37] P. Martini, A. Schulz, and H. Bauer, “Film Cooling Effectiveness and Heat Transfer on the Trailing–edge Cutback of Gas Turbine Airfoils with Various Internal Cooling,” *J. Turbomach.*, vol. 128, pp. 196–205, 2006.

[38] G. Barigozzi, A. Armellini, C. Mucignat, and L. Casarsa, “Experimental Investigation of the Effects of Blowing Conditions and Mach Number on the Unsteady Behavior of Coolant Ejection through a Trailing–edge Cutback,” *J. Heat and Fluid Flow*, vol. 37, pp. 37–50, 2012.

[39] S. Ravelli and G. Barigozzi, “Application of Unsteady Computational Fluid Dynamics Methods to Trailing–edge Cutback Film Cooling,” *J. Turbomach.*, vol. 136, no. 12, p. 121006, 2014.

[40] S. Ravelli and G. Barigozzi, “Dynamics of Coherent Structures and Random Turbulence in Pressure Side Film Cooling on a First Stage Turbine Vane,” *J. Turbomach.*, vol. 141, no. 1, p. 11003, 2018.

[41] S. Ravelli and G. Barigozzi, “Stress-Blended Eddy Simulation of Coherent Unsteadiness in Pressure Side Film Cooling Applied to a First Stage Turbine Vane,” *J. Heat Transfer*, vol. 140, pp. 92201–14, 2018.

[42] P. Martini and A. Schulz, “Experimental and Numerical Investigation of Trailing–edge Film Cooling by Circular Coolant Wall Jets Ejected From a Slot with Internal Ribs Arrays,” *J. Turbomach.*, vol. 126, pp. 229–236, 2004.

[43] H. Schneider, D. von Terzi, and H. J. Bauer, “Large-Eddy Simulations of Trailing-edge Cutback Film Cooling at Low Blowing Ratio,” *J. Heat and Fluid Flow*, vol. 31, no. 5, pp. 767–775, 2010.

[44] H. Schneider, D. A. Von Terzi, H. J. Bauer, and W. Rodi, “Coherent Structures in Trailing-edge Cooling and the Challenge for Turbulent Heat Transfer Modelling,” *J. Heat and Fluid Flow*, vol. 51, pp. 110–119, 2015.

[45] M. E. Taslim, S. D. Spring, and B. P. Mehlman, “Experimental Investigation of Film Cooling Effectiveness for Slots of Various Exits Geometries,” *J. Thermophys. Heat Transf.*, vol. 6, no. 2, pp. 302–307, 1992.

[46] M. Effendy, Y. F. Yao, J. Yao, and D. R. Marchant, “DES Study of Blade Trailing–edge Cutback Cooling Performance with Various Lip Thicknesses,” *J. Appl. Therm. Eng.*, vol. 99, pp. 434–445, 2016.

[47] J. Hwang and C. Lui, “Detailed Heat Transfer Characteristic Comparison in Straight and 90-deg Turned Trapezoidal Ducts with Pin-fin Arrays,” *J. Heat Mass Transf.*, vol. 42, pp. 4005–4016, 1999.

[48] J. Hwang and C. Lui, “Measurement of Endwall Heat Transfer and Pressure Drop in a Pin-fin Wedge Duct,” *J. Heat Mass Transf.*, vol. 45, pp. 877–889, 2002.

[49] L. Tarchi, B. Facchini, and S. Zecchi, “Experimental Investigation of Innovative Internal Trailing–edge Cooling Configurations with Pentagonal Arrangement and Elliptic Pin–fin,”.

J. Rotating Mach., 2008.

[50] R. J. Goldstein and S. B. Chen, "Flow and Mass Transfer Performance in Short Pin-Fin Channels with Different Fin Shapes," *J. Rotating Mach.*, vol. 4, no. 2, pp. 113–128, 1998.

[51] D. E. Metzger, R. A. Berry, and J. P. Bronson, "Developing Heat Transfer in Rectangular Ducts with Staggered Arrays of Short Pin–Fins," *J. Heat Transfer*, vol. 104, no. 4, pp. 700–706, 1982.

[52] G. Liao, X. Wang, J. Li, and F. Zhang, "A Numerical Comparison of Thermal Performance of In-line Pin–fins in a Wedge Duct with Three Kinds of Coolant," *J. Heat Mass Transf.*, vol. 77, pp. 1033–1042, 2014.

[53] M. Moon and K. Kim, "Analysis and Optimization of Fan–shaped Pin–fin in a Rectangular Cooling Channel," *J. Heat Mass Transf.*, vol. 72, pp. 148–162, 2014.

[54] F. E. Ames, L. A. Dvorak, and M. J. Morrow, "Turbulent Augmentation of Internal Convection Over Pins in Staggered Pin–fin Arrays," *J. Turbomach.*, vol. 127, no. 1, pp. 183–190, 2005.

[55] F. E. Ames and L. A. Dvorak, "Turbulent Transport in Pin–fin arrays: Experimental Data Predictions," *J. Turbomach.*, vol. 128, no. 1, pp. 71–81, 2006.

[56] M. Axtmann, R. Poser, J. Von Wolfersdorf, and M. Bouchez, "Endwall Heat Transfer and Pressure Loss Measurements in Staggered Arrays of Adiabatic Pin–fins," *J. Appl. Therm. Eng.*, vol. 103, pp. 1048–1056, 2016.

[57] D. A. von Terzi, R. D. Sandberg, and H. F. Fasel, "Identification of Large Coherent Structures In Supersonic Axisymmetric Wakes," *J. Comput. Fluids*, vol. 38, no. 8, pp. 1638–1650, 2009.